Original paper

Development and assessment of 3D-printed individual applicators in gynecological MRI-guided brachytherapy

Helena Barbara Zobec Logar, MD, MSc[1,2], Robert Hudej, PhD[1], Barbara Šegedin, MD, Assist. Prof.[1,2]

[1]Department of Radiation Oncology, Institute of Oncology Ljubljana, Ljubljana, Slovenia, [2]Medical Faculty, University of Ljubljana, Ljubljana, Slovenia

Abstract

Purpose: To evaluate the clinical use of 3D printing technology for the modelling of individual applicators for advanced gynecological tumors in magnetic resonance imaging (MRI)-based brachytherapy (BT).

Material and methods: We tested individually designed 3D-printed applicators in nine patients with advanced gynecological cancer. Before BT was performed, all patients were treated with external beam radiotherapy (EBRT). The most common indication for individualized BT was advanced gynecological tumors where the use of standard BT applicators was not feasible. Other indications were suboptimal dose-volume histogram (DVH) parameters for high-risk clinical target volume (CTV-T_{HR}) at the first BT ($V_{100} \leq 90\%$ of CTV-T_{HR} volume and $D_{98} \leq 80\%$, $D_{90} \leq 100\%$, and $D_{100} \leq 60\%$ of dose aim). The EQD_2 dose aim to the target volume D_{90} CTV-T_{HR} per one BT fraction was 20 Gy for cervical or recurrent endometrial cancer and 16 Gy for vaginal cancer patient. The first BT with the standard applicator *in situ* was used as the virtual plan for designing a 3D-printed applicator. The next BT was performed with a 3D-printed applicator *in situ*. The primary endpoint was to improve CTV-T_{HR} DVH parameters without exceeding the dose to the organs at risk (OARs).

Results: All DVH parameters for CTV-T_{HR} were significantly higher with the use of an individually designed applicator. Mean D_{90} CTV-T_{HR} improved from 14.1 ±5.4 Gy to 22.0 ±2.5 Gy and from 7.1 Gy to 16.2 Gy for cervical/recurrent endometrial and vaginal cancer, respectively ($p < 0.001$). The mean D_{2cm^3} bladder, rectum, sigmoid, and bowel dose was within institutional dose constraints, and increased from 13.0 ±1.5 Gy to 13.6 ±1.5 Gy ($p = 0.045$), 10.8 ±1.2 Gy to 11.7 ±1.3 Gy ($p = 0.004$), 8.9 ±3.2 Gy to 10.3 ±3.3 Gy ($p = 0.008$), and 8.7 ±3.8 Gy to 9.2 ±3.1 Gy ($p = 0.2$).

Conclusions: With the use of individual 3D-printed applicators, all DVH parameters for CTV-T_{HR} significantly improved without compromising the dose constraints for the OARs.

J Contemp Brachytherapy 2019; 11, 2: 128–136
DOI: https://doi.org/10.5114/jcb.2019.84741

Key words: image-guided brachytherapy, 3D printing, gynecological cancer.

Purpose

Image-guided adaptive brachytherapy (IGABT) is crucial for the treatment of advanced gynecological cancers [1,2,3,4,5]. The benefits of the combined intracavitary/interstitial (IC/IS) approach in advanced cervical cancer brachytherapy (BT) have already been demonstrated [6,7,8,9,10,11]. Standard applicators, such as Vienna-type ring applicator or Utrecht-type ovoid applicator, do not enable an adequate coverage of the target volume in all patients with advanced cervical cancer [3,12,13]. The 3D printing technology show promising results in different aspects of medical science and also in radiation oncology [14,15,16,17,18,19,20,21,22]. Patient specific boluses for radiotherapy can be designed for irregular surfaces to improve dose distribution. It is an attractive method for in-hospital design and modeling of BT applicators for skin, head and neck, breast, prostate, and gynecological cancers. Complex implantations can be performed, and accurate dose delivery can be achieved with individual template-guided procedures. This is of special importance in head and neck cancer due to the proximity of organs at risk (OARs). The process of manufacturing customized applicators is fast and financially viable. 3D printing technologies commonly used in medicine are stereolithography (SLA) and selective laser sintering (SLS). Different magnetic resonance imaging (MRI) compatible materials, in the form of a powder, liquid resin, or photopolymers, registered for use in medicine, are available and can be applied in BT. The material used determines the applicator's properties. The final product needs to be firm and have a smooth surface.

Address for correspondence: Helena Barbara Zobec Logar, MD, MSc, Institute of Oncology Ljubljana, Zaloška 2, 1000 Ljubljana, Slovenia, phone: +386 15879204, e-mail: hlogar@onko-i.si

Received: 18.11.2018
Accepted: 29.03.2019
Published: 29.04.2019

The most important aspects of 3D-printed applicators are suitability for patient's anatomy, better needle guidance, improved target coverage, and less trauma to the surrounding tissue and OARs. Consequently, smaller dose applied to OARs and reduced toxicity are expected. A better target coverage can be translated in higher tumor control probability [4,13,23,24,25,26,27].

We started using 3D printing technology for individual BT applications in 2015 [20]. In this paper, we present the results of a single-institution, one arm, non-randomized feasibility study on 3D-printed applicators for individualized gynecological cancer BT.

Material and methods

Nine patients were included in the study, and they were treated with external beam radiotherapy (EBRT) using volumetric modulated arc therapy (VMAT) or intensity modulated radiation therapy (IMRT) to 45-50 Gy prescribed in 25-28 fractions. Patients and tumor characteristics are presented in Table 1. Patients received concomitant cisplatin-based chemotherapy, 40 mg/m^2 once per week in case of cervical or vaginal cancer. Carboplatin was used in case of renal dysfunction. EBRT was followed by two BT fractions. An additional BT insertion with standard IC applicator, usually in paracervical anesthesia, was performed in six patients with large-volume tumors or a narrow vagina one week before first BT treatment for virtual planning. In the remaining three patients, MR images from the first BT treatment with the standard IC/IS applicator in place were used for virtual planning if the dose parameters from the plan were suboptimal.

Patients were treated with PDR GammaMed Plus iX afterloader (Varian Medical Systems). The dose aim to the target volume D_{90} high-risk clinical target volume (CTV-T_{HR}) was 15.0 Gy in 22 pulses for vaginal cancer and 18.5 Gy in 25 pulses for cervical or recurrent endometrial cancer, with usually one week between fractions. Imaging with the applicator *in situ* was performed with GE Optima MR450w 1.5T MRI scanner. T2-weighted fast spin-echo sequence with a voxel size of 0.6 × 0.6 × 3.6 mm, and 3D isotropic T2-weighted fast spin-echo sequence with a voxel size of 1.0 × 1.0 × 1.0 mm were used. Contouring and treatment planning were performed in the BrachyVision treatment planning system (Varian Medical Systems).

Patient selection

Patients with locally advanced primary or recurrent cervical, endometrial, and vaginal cancer were eligible for the study. In the process of patients' selection for individualized BT, several factors were taken into consideration. The most important of these was the extent of primary tumor (parametrial or paravaginal extension, involvement of sacrouterine ligament, pararectal space, or adjacent organs). Other factors were anatomical characteristics such as narrow vagina not suitable for standard applicator insertion, or the proximity of blood vessels. The following factors obtained from the plan using a standard BT applicator were also considered as an indication for the use of individualized applicator: exceeded dose to OARs and suboptimal dose-volume parameters for CTV-T_{HR} ($V_{100} \leq 90\%$ of the CTV-T_{HR} volume and $D_{98} \leq 80\%$, $D_{90} \leq 100\%$, and $D_{100} \leq 60\%$ of the dose aim to D_{90} CTV-T_{HR}).

Virtual plan and modelling of individual applicators

Plan A was a virtual plan and the starting point for 3D individual applicator construction. It was based on MRI from the first BT application, with the standard applicator *in situ*. The standard applicator for primary cervical and vaginal cancer of the upper part of vagina was a tandem and ring applicator, with a cap add-on for parallel interstitial needles (Vienna-type ring applicator). In patients after hysterectomy, a ring with a cap for parallel needles or a vaginal cylinder was used as the standard applicator [28]. CTV-T_{HR}, gross tumor volume (GTV-T), and OARs were delineated on MRI. The same concept for the target volume definition and delineation as for cervical cancer was transferred to vaginal and recurrent endometrial or recurrent cervical cancer. CTV-T_{HR} was defined as palpable mass at the time of BT and all grey zones visible on T2-weighted MRI. GTV-T was included in CTV-T_{HR}

Table 1. Patients and tumor characteristics

Characteristics	*n*
Age (years), median (range)	59 (28-75)
Tumor type	
Cervical cancer	7
Endometrial cancer	1
Vaginal cancer	1
Histology	
Squamous cell carcinoma	7
Adenocarcinoma	2
Stage	
Cervical cancer stage IIIb*	5
Recurrent cervical cancer	2
Recurrent endometrial cancer	1
Vaginal cancer stage IVa*	1
Chemotherapy	
Cisplatin 40 mg/m^2 (≥ 2 cycles)	5
Carboplatin AUC 1.5 (5 cycles)	1
None	3

*AUC – area under the curve, *International Federation of Gynecology and Oncology (FIGO) staging system for cervical and vaginal cancer*

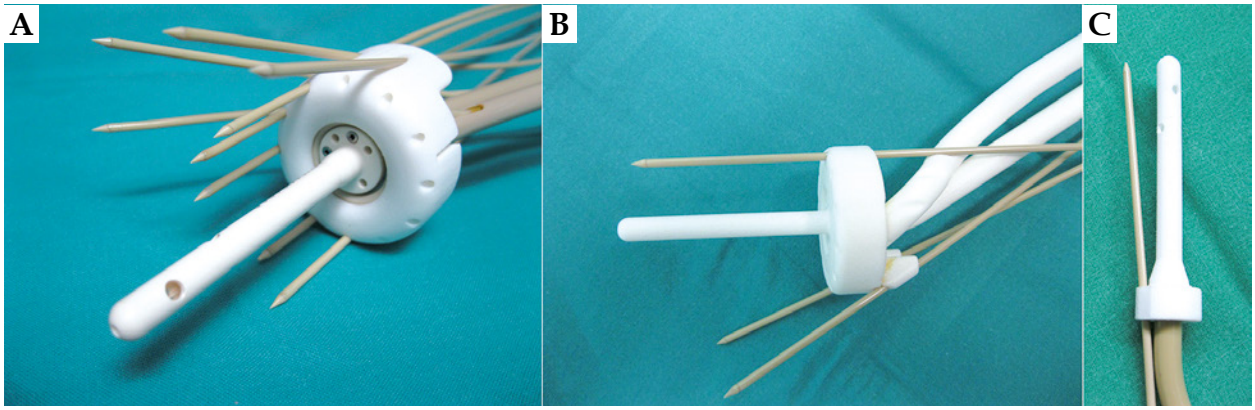

Fig. 1. A) 3D-printed add-on for the ring with parallel and oblique needles. If 3D-printed cap add-on is used, the outside diameter of the ring is increased by 7 mm; **B**) 3D-printed tandem and ring. The size of the ring can be adjusted to the diameter of the vagina, and an oblique needle insertion at an angle of up to 45 degrees is possible; **C**) 3D-printed tandem with a needle inserted at a 15-degree angle

and was defined as macroscopic tumor (visible and/or palpable mass) at the time of BT and high signal regions on T2-weighted MRI.

Parallel and oblique needle positions were adapted to the tumor volume. The exact needle entry point location, angle, and depth of insertion into the tissue were defined for each needle. The angle of oblique needle insertion was defined as the angle between the tandem axis and the needle axis, or in patients after hysterectomy as the angle between the ring or vaginal cylinder central axis and the needle axis. The aim of plan A was optimal CTV-T_{HR} coverage. In this step, the dose to OARs was allowed to exceed the dose constraints due to OARs inter-fraction variability. In the next step, standard applicator model was individually adapted by adding needle guiding holes according to plan A.

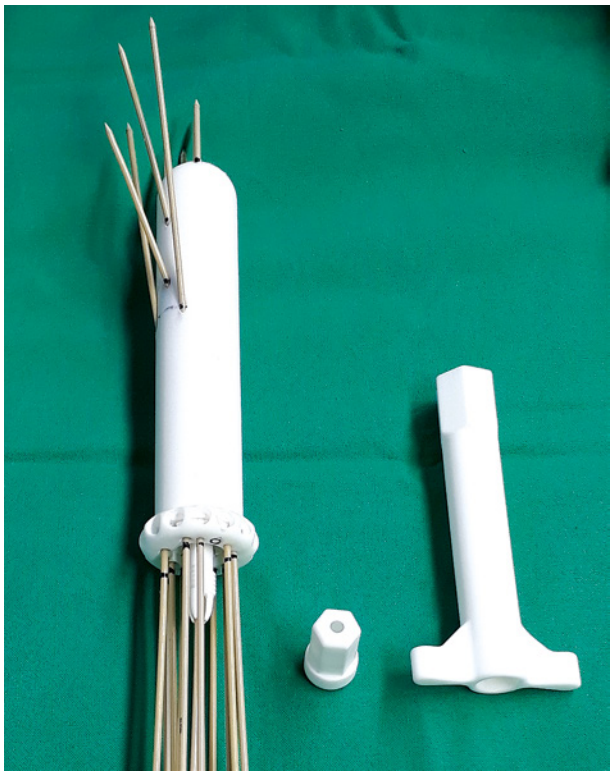

Fig. 2. 3D-printed multi-channel vaginal cylinder with intracavitary/interstitial needles. Appropriate for narrow vagina and multiple vaginal lesions. A handle (right) is used to tighten the nut (middle) on the collect chuck of the cylinder for needle fixation. It is used at the end of application to fix all the needles at the same time

Several types of individual applicators were designed. In 5 patients with cervical cancer, a tandem plus ring with a 3D-printed add-on for parallel and oblique needles was used. In 3 patients with recurrent cervical or endometrial cancer after hysterectomy, a ring with 3D-printed add-on was used. In one patient with vaginal cancer, a multichannel cylinder was used. Some solutions are presented in Figures 1 and 2. In narrow vagina, two applicator designs were proposed. The first design was a ring-shaped applicator, with twelve holes on the ring circumference for the parallel needles. Dwell positions in the needles at the level of the ring were used as a replacement of dwell positions in the active channel of Vienna-type ring applicator. The second design was a multi-channel vaginal cylinder (Figure 2).

3D modeling and 3D printing of individual applicators was outsourced to a company registered for the manufacturing of medical devices with SLS technology. For the applicator production, a biocompatible polyamide PA2200 material was used, and the applicators were printed using a Formiga P100 3D printer. The applicator was delivered and sterilized 6 days after plan A. The treatment time was not prolonged due to the use of an individual applicator. There were no intra- and perioperative complications.

Brachytherapy procedure and treatment planning

Before the first use of the 3D-printed ring applicator, a Varian bronchial catheter was inserted in the ring channel. Similarly, Varian guiding tube catheter was inserted in the tandem or vaginal cylinder central channel. Varian catheters were used to connect the applicators to the afterloader. In this way, it was ensured that the source capsule was always

in contact only with Varian certified materials. As part of the quality control, the applicators were scanned on computer tomography (CT) in order to measure their internal structure. Additionally, active channel patency and geometry of the needle guiding holes were carefully checked.

At the time of BT, the exact needle insertion length was marked on the needle with a sterile marker before the applicator insertion. After the applicator insertion, parallel and oblique needles were inserted one by one through guiding holes to predefined depth. Their position was checked with transrectal and transabdominal ultrasound. The individual applicators were fixed in the same way as the standard applicators with vaginal tamponade and adhesive tape. The fixation of the needles in multichannel vaginal cylinder was performed with a handle at the end of the application (see explanation in Figure 2). Water-filled catheters were inserted into the ring and tandem applicators or in the central channel of the vaginal cylinder in order to visualize the applicator active channel on T2-weighted MR images. The same technique for the applicator reconstruction was used both in standard and individual applicators, in agreement with the GEC-ESTRO GYN recommendations on applicator reconstruction [29].

After applicator insertion, MRI scanning was performed. CTV-T_{HR}, GTV-T, and OARs were delineated, and the *in situ* applicator was reconstructed on MRI images. In the tandem and ring applicator, the starting point for dose optimization was standardized pear-shaped dose distribution with dose normalized to point A. The dwell times in the needles were normally limited to 20% of the dwell times of the standardized plan in order to prevent dose hot spots. In individual cases, the dwell time limit was increased to 30% of the standardized dwell times to compensate for suboptimal implant geometry. Dose optimization was performed in iterative steps by changing dwell positions and dwell times in the IC and IS parts of the implant. Reiteration was performed until the dose constraints for CTV-T_{HR} and OARs were met. In a multi-channel cylinder, the central channel dwell positions were loaded first, and the prescribed dose was normalized to the applicator surface in the central plane of the cylinder. Afterwards, dwell positions of the needles were loaded to cover the target volume with the prescribed dose. For the purpose of vaginal mucosa sparing, the needles were loaded at least 5 mm from the vaginal surface into the tissue. Three different types of individual implants are displayed in Figure 3.

The cumulative dose aim (EBRT + 2 BT fractions) to the CTV-T_{HR} was D_{90} > 85 Gy EQD_2 for cervical or recurrent endometrial cancer, and 82 Gy for vaginal cancer patient. For OARs, the D_{2cm^3} EQD_2 constraints were as follows: rectum, sigmoid, and bowel 70 Gy, and bladder 75 Gy. EQD_2 was calculated using $\alpha/\beta = 10$ for tumor and $\alpha/\beta = 3$ for OARs. The estimated repair half-time for PDR was 1.5 hours. The aim per one BT fraction was CTV-THR V_{100} > 90% of the CTV-T_{HR} volume, and D_{98} > 80%, D_{90} > 100%, and D_{100} > 60% of the prescribed dose to D_{90} CTV-T_{HR}. Assuming an EBRT dose of 45 Gy with 1.8 Gy/fraction, the D_{2cm^3} constraints for a single BT fraction were 15.1 Gy for the bladder and 13.4 Gy for the rectum, sigmoid, and bowel. If an EBRT dose of 50 Gy, 2 Gy/fraction was delivered, the D_{2cm^3} constraints for a single BT fraction were 12.5 Gy for the bladder and 10.6 Gy for the rectum, sigmoid, and bowel.

For each patient, DVH parameters of three plans were compared: the virtual plan for designing individual applicator (plan A), the plan with the standard IC/IS applicator (plan B), and the plan with individual applicator (plan C). Plan A was created from the MRI from the first BT application, with standard applicator *in situ*. Virtual needles were introduced in the treatment planning system to obtain the best possible coverage of the CTV-T_{HR}, taking into account anatomical and geometrical limitations of the applicator. Plan A was never used for treatment. Plan C was created using the MRI from the second BT, with an individual applicator *in situ*. Plan B was created using the same MRI as plan C and a standard applicator. Standard applicator for plan B was defined as an individual applicator without oblique needles. Standard applicator for plan B for cervical cancer with uterus *in situ* was tandem and ring with parallel needles; for hysterectomized patient (recurrent endometrial, cervical, or vaginal cancer), the standard applicator was ring or vaginal cylinder with parallel needles. Plan B was not used for treatment either.

Statistics

The data were analyzed using IBM SPSS statistical software package version 23.0 (SPSS Inc., Chicago, IL, USA). *P* values of < 0.05 were considered statistically

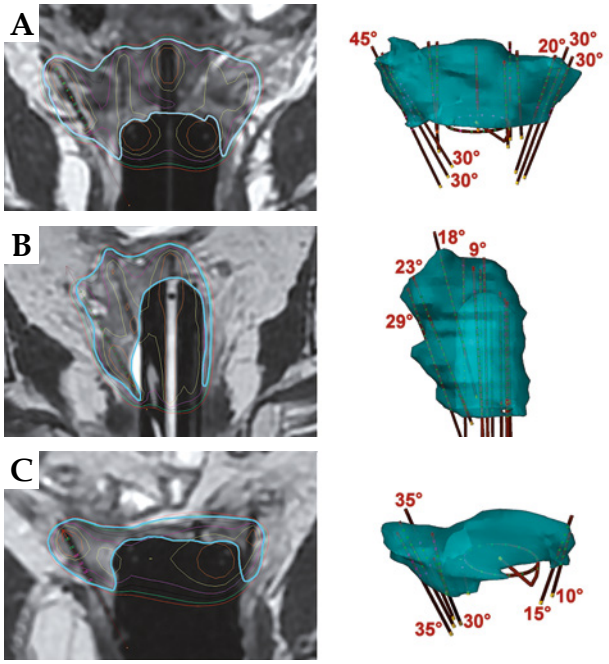

Fig. 3. MRI of three different types of 3D implants (left side) with corresponding CTV-T_{HR} (cyan color), with active channel source positions and angles for oblique needles (right side). **A**) Tandem, ring, and add-on for parallel and oblique needles; **B**) Multi-channel vaginal cylinder for the implantation of parallel and oblique needles; **C**) Ring for the interstitial implantation of parallel and oblique needles; **B** and **C**) Implants used in patients after hysterectomy

significant. The paired-sample *t*-test or Wilcoxon signed-rank non-parametric test for related samples was performed to test the difference.

The study was approved by the Republic of Slovenia National Medical Ethics Committee (approval number: 0120-282/2016-2) and by the Protocol Review Board at the Institute of Oncology Ljubljana (ERID-KESOPKR/63), and was in agreement with the Declaration of Helsinki. All the patients signed an informed consent form. The study was registered in the ClinicalTrials.gov database (NCT03466957).

Results

In our study, the mean number of needles that were used in the individual applicator was 9 ±2. The mean number of parallel needles was 5 ±2, and the mean number of oblique needles was 4 ±2 at 10 to 45-degree angle. The mean depth of needle implantation was 4 ±1.4 cm, for parallel needles 3 ±1.2 cm, and for oblique needles 4 ±1.4 cm. The maximal depth of needle implantation was 6.8 cm. The parallel needles were most often implanted in the 4-11 o'clock (clockwise) ring positions, while oblique needles were implanted in the 4-5 and 9-10 o'clock ring positions corresponding to the sites of the tumor infiltration.

DVH parameters for all three plans of all patients per one BT fraction are presented in Table 2. All DVH parameters for CTV-T_{HR} were markedly improved with the use of individually designed 3D-printed applicators (Figure 4). If plan B was compared to plan C, all CTV-T_{HR} parameters (CTV-T_{HR} V_{100}, D_{98}, D_{90}, and D_{100}) and GTV-T D_{98} significantly improved ($p < 0.001$ for CTV-T_{HR} D_{90}, V_{100}, D_{98}, and D_{100}; $p = 0.007$ for GTV-T D_{98}). They resulted in an increased mean CTV-T_{HR} DVH parameters: 22.3 ±13.4% for V_{100}, 46.9 ±20.9% for D_{98}, 44.6 ±26.7% for D_{90}, 32.0 ±15.9% for D_{100}, and 33.7 ±27.9% for GTV D_{98}. CTV-T_{HR} V_{100}, D_{98}, D_{90}, and D_{100} were ≥ 93.1%, ≥ 80.6%, ≥ 103.6%, and ≥ 37.4% in all patients, respectively. GTV-T D_{98} was more than 105% of the prescribed dose in all cases. Each CTV-T_{HR} DVH parameter in plan C had a smaller standard deviation compared to plan B.

As expected, the difference in DVH parameters between plan A and plan C was non-significant ($p > 0.05$). In most cases, the DVH parameters for CTV-T_{HR} in plan A were the best that could be achieved for CTV-T_{HR} coverage in a given patient, partly because no special consideration was given to OARs. The primary aim of plan A was the improvement of spatial distribution of parallel and oblique needles in order to obtain the best possible CTV-T_{HR} coverage and not the dose to OARs. The difference between DVH parameters in favor of plan A for CTV-T_{HR} D_{98}, D_{90}, V_{100}, D_{100}, and GTV-T D_{98} were 3.4 ±16.2%, 5.6 ±12.7%, 1.3 ±3.5%, 0.2 ±9.0%, and 27.3 ±33.9%, respectively. The dose constraints for OARs were exceeded in most cases (6/9 patients) in plan A, while respected in all patients in plan B and in most patients in plan C. The mean increase in the dose constraints for D_{2cm^3} per one BT fraction for the bladder, rectum, sigmoid and bowel when comparing plans C and B was 4.3 ±5.5%, 6.6 ±4.9%, 10.7 ±9.1%, and 4.4 ±9.2%, respectively ($p < 0.05$ for the bladder, rectum, and sigmoid; $p = 0.2$ for the bowel). The mean increase in the dose constraints for D_{2cm^3} per one BT fraction between plan A and C for the bladder, rectum, sigmoid and bowel was 15.2 ±12.2%, 26.1 ±38.9%, 10.6 ±30.9%, and 34.2 ±27.9%, respectively ($p < 0.05$ for bladder and bowel; $p > 0.05$ for rectum and sigmoid). In two patients, the dose to the bladder and rectum slightly increased with the use of individual applicators (plan C), without surpassing the cumulative EBRT + 2 BT EQD_2 dose.

The mean volume of CTV-T_{HR} was 49.9 ±31.1 cm^3. The lowest CTV-T_{HR} volume was only 5.2 cm^3 in a patient with recurrent cervical cancer after hysterectomy, and the highest was 96.7 cm^3 in a patient with primary cervical cancer. The benefit of individual applicators was seen in both small and large tumor volume, and was strongly related to the topography of the tumor. In Figure 5, the relation between percentage of the dose constraints to OARs and percentage of the prescribed dose to CTV-T_{HR} D_{90} is visualized for all OARs. Plan C offered optimal results for CTV-T_{HR} coverage in relation to the dose to OARs. CTV-T_{HR} was well covered in plan A, but the dose to OARs was exceeded in 6/9 of these patients for bladder, in 5/9 for rectum, and in 4/9 for sigmoid and bowel. OARs dose constraints were met in plan B, except for one patient, while CTV-T_{HR} was underdosed for all patients, except one.

Discussion

IGABT has become a standard of care in patients with advanced cervical cancer. It has significantly improved local and pelvic control rates for all cervical cancer stages, with a survival benefit of at least 10%. Major morbidity was decreased by about 50% [1,4,5]. The 3D printing technology is a promising new approach in IGABT and offers the possibility of improving standard BT applicators available on the market as well as developing new ones. A potential benefit of 3D printing technology is to escalate the dose to the target and de-escalate the dose to OARs. 3D-printed applicators are useful tools for guiding needle implantation at different angles and directions. Freehand needles can be used as well, but it is difficult to implant them accurately at predefined angels and to a certain location. However, only a limited number of reports on the use of 3D technology in BT have been published up to date [14,15,17,20,21,30,31]. For intact cervical cancer, CTV-T_{HR} D_{90} dose of ≥ 85 Gy in 7 weeks leads to 3-year local control rates of > 86% in large size CTV-T_{HR} and > 93% in intermediate size CTV-T_{HR}. In advanced tumors, appropriate target coverage can only be achieved with combined IC/IS application [1,4,6,7,9,13,32]. RetroEmbrace study outcomes showed that the dose to CTV-T_{HR} in cervical cancer decreased significantly with advanced stage from the mean D_{90} of 93 Gy in stage IB to 78 Gy in stage IVA [1]. It was also shown that half of the patients with volumes CTV-T_{HR} of more than 30 cm^3 received doses of less than 85 Gy [33]. Suboptimal local control is predicted if the dose to CTV-T_{HR} is less than 85 Gy. A further study demonstrated that a dose escalation from 75 Gy to 85 Gy resulted in increased local control of 3%

Table 2. DVH parameters for CTV-T_{HR} (**A**) and OARs (**B**) for one BT fraction. The dose prescribed to D_{90} CTV-T_{HR} was 18.5 Gy for cervical or recurrent endometrial cancer, or 15 Gy for vaginal cancer patient (patient 9). Mean and standard deviation (SD) values are reported. The dose to OARs is presented as the percentage of the dose constraints. Assuming an EBRT dose of 45 (50) Gy with 1.8 (2) Gy/fraction, the D_{2cm^3} constraints for a single BT fraction are 15.1 (12.5) Gy for bladder and 13.4 (10.6) Gy for rectum, sigmoid, and bowel. If the OAR (bowel) was not visible on MRI images, the cell is empty

A

Patient	CTV-T_{HR} D_{98} (%)			CTV-T_{HR} D_{90} (%)			CTV-T_{HR} V_{100} (%)			CTV-T_{HR} D_{100} (%)			GTV-T D_{98} (%)			CTV-T_{HR}
	Plan A	Plan B	Plan C	Plan A	Plan B	Plan C	Plan A	Plan B	Plan C	Plan A	Plan B	Plan C	Plan A	Plan B	Plan C	V (cm^3)
1	106.3	50.8	80.6	127.8	70.7	108.8	99	77.9	93.2	63.8	24.3	54.6	138.9	63.3	105.2	73.1
2	92.7	55.1	85.4	110.3	74.3	108.1	95.4	70.9	93.8	71.9	42.2	64.3	129.1	83.5	127.9	59.6
3	110.3	38.8	111.9	130	48.7	137.5	99.4	63.4	99.6	71.4	30.8	87.0	162.5	113.3	110.5	5.2
4	97.8	32	106.2	117.2	50.3	121.9	97.5	65.4	99.1	73.5	23.2	74.6	134.2	40.2	118.2	16.9
5	98.7	67.4	103.3	120	98.5	116.8	97.7	89.2	98.9	72.4	42.7	74.1	155.3	79.2	119	65
6	112.4	67.6	118.7	139.5	125.5	140.3	99.6	95.3	99.7	81.6	40.5	69.7	166.6	175.4	179.6	24.6
7	111.6	26.9	89.4	131.9	43.8	103.6	99.3	61.2	93.1	38.4	12.3	37.4	207.9	99.9	109.8	51.8
8	90.3	81.1	94.9	113.8	99.2	115.2	96.2	89.6	97	53.4	56.2	59.0	126.4	110.2	131.3	96.7
9	105.5	34.7	86.9	124.1	47.2	107.7	99.1	55.4	94.3	64.7	24.0	63.3	135.5	42	109.2	56.4
Mean	102.8	50.5	97.5	123.8	73.1	117.8	98.1	74.3	96.5	65.7	32.9	64.9	150.7	89.7	123.4	49.9
SD	8.3	18.8	13.1	9.4	29.0	13.2	1.5	14.4	2.9	12.9	13.5	14.1	25.9	41.8	22.8	29.2

B

Patient	Bladder D_{2cm^3} (%)			Rectum D_{2cm^3} (%)			Sigmoid D_{2cm^3} (%)			Bowel D_{2cm^3} (%)		
	Plan A	Plan B	Plan C	Plan A	Plan B	Plan C	Plan A	Plan B	Plan C	Plan A	Plan B	Plan C
1	117.2	91.4	92.7	89.6	88.1	83.6	35.8	82.1	92.5	129.9	97.0	98.5
2	102.0	94.0	100.7	111.9	86.6	94.8	101.5	77.6	92.5	24.6	47.0	49.3
3	97.4	91.4	88.7	56.0	72.4	75.4	112.7	76.9	87.3	78.4	43.3	44.8
4	90.1	82.1	83.4	67.9	76.9	88.8	53.0	35.1	29.1	135.1	88.1	79.9
5	95.4	67.5	70.9	132.8	73.9	79.9	124.6	93.3	94.8	147.8	93.3	92.5
6	101.3	90.1	91.4	129.1	70.1	81.3	88.8	76.9	94.0		82.8	87.3
7	137.7	81.5	98.0	207.5	98.5	106.7	103.7	47.0	69.4	107.5	44.0	56.0
8	108.6	98.7	102.6	100.0	82.8	91.8	77.6	81.3	87.3			
9	115.2	92.8	100.0	144.3	95.3	101.9	98.1	34.0	53.8	89.6	30.2	52.8
Mean	107.2	87.7	92.1	115.5	82.7	89.3	88.4	67.1	77.9	101.8	65.7	70.1
SD	14.5	9.3	10.1	45.4	10.2	10.5	28.6	22.2	22.9	42.2	27.0	21.6

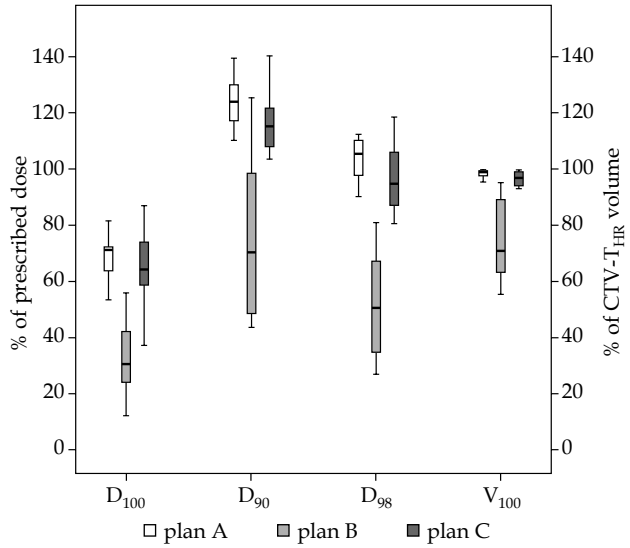

Fig. 4. DVH parameters for CTV-T_{HR} D_{90}, D_{98}, and D_{100} in percentage of prescribed dose to D_{90} CTV-T_{HR} and V_{100} in percentage of CTV-T_{HR} volume. The dose prescribed to D_{90} CTV-T_{HR} was 18.5 Gy or 15 Gy per fraction in vaginal cancer patient (patient 9, Table 2). **A**) Plan A: virtual plan for designing individual applicator; **B**) Plan B with standard applicator; **C**) Plan C with 3D-printed individual applicator

in limited/intermediate size volume, and of 7% in large size volume CTV-T_{HR} [13]. It was proved that combined IC/IS technique improves the therapeutic ratio in locally advanced cervical cancer. IS technique is an optimal solution for boosting involved parametrium [12].

In our study, the principles for cervical cancer IC/IS approach were used also for other gynecological cancers. With individual applicators, the mean D_{90} to CTV-T_{HR} in all patients increased by 44.6 ±26.7% compared to standard applicator. According to the local tumor control probability (TCP) model, about 15% better local control at 3 years due to the increment in the dose can be expected in patients with locally advanced cervical cancer [13]. On the other hand, the dose to OARs in most of the cases was below institutional dose constraints, which were lower than those used in most other IGABT studies, except for the rectum within the dose limits proposed in the EMBRACE II study [3,4,32,33,34]. It was shown that the rectal dose of ≥ 75 Gy is associated with a 12.5% risk of fistula at 3 years, and the dose of ≤ 70 Gy limited G2-G4 proctitis to ≤ 10.2% [35]. Findings from the Embrace I study suggest limiting the bladder D_{2cm^3} to ≤ 80 Gy [33]. With dose constraints for the bladder in our study, the probability of G2-G4 bladder late morbidities was estimated to be up to about 20% [36]. With the sigmoid and bowel dose limit for D_{2cm^3} < 70 Gy, no additional side effects are to be expected apart from those mentioned in other studies [4,33,34]. The mean percentage of the dose constraints for D_{2cm^3} per one BT fraction was 92.1 ±10.1 for the bladder and 89.3 ±10.5 for the rectum. If the two BT fractions with the same dose were to be delivered to both fractions, the dose to OARs would still be below the dose constraints proposed for OARs.

However, there are some limitations of the method and study. An individualized 3D-printed approach is needed for a minority, in our experience about 5%, of patients with gynecological cancers (primary or recurrent cervical, endometrial or vaginal cancer), who are candidates for BT. For the majority of patients, the standard IC/IS applicators offer optimal results for the target coverage.

Based on the results from this study, the benefit of using individual applicators is to be expected for all stages and for all tumor volumes. It is not reliant only on the tumor volume or the tumor stage, but also on the anatomy of the tumor and nearby structures (proximity of OARs, blood vessels, narrow vagina, etc.). Patients with both small and large tumors would benefit from individual applicators due to difficult topography. The important step in designing the individual applicator is choosing the right type of standard applicator that suits the patient's anatomy and tumor's topography. Three types of standard applicators were used in our study: in patients with uterus *in situ*, a tandem with a ring or a multichannel vaginal cylinder with a tandem, and in hysterectomized patients, a ring or a cylinder depending on the tumor extension to vagina. The next important step is reproducing the applicator position for all insertions. If the patient has a uterus, the uterine channel facilitates reproducible applicator positioning in all applicator insertions. Consequently, it is more difficult to position the applicator in hysterectomized patients. Ultrasound can be useful for the purpose of accurate applicator positioning.

Future improvement of the technique would be the development of a computer program that would automate the design of individualized applicator. With the help of a dedicated software, the standard type of applicator inserted into the patient would be chosen from the library of applicators. Based on the target and OARs delineated on the MRI, virtual needles would be added to the standard applicator, resulting in an individual applicator. Such an automated process would speed up the design of individualized applicator. It would also enable optimal applicator geometry for each individual patient.

Patients anatomically unsuitable for the use of individual BT applicators are candidates for the perineal template BT, other techniques (EBRT boost, intraoperative BT, stereotactic, or proton therapy) may be considered as well [37,38,39,40]. The process of manufacturing individual applicators is not automated and demands skillful and dedicated staff. Moreover, not all materials on the market designated for the use in medicine have proper characteristics for an applicator's production. The weakness of our study is also a low number of the patients, which is mainly due to the eligibility criteria.

Conclusions

This study focused on designing and testing 3D-printed applicators for clinical practice. We confirmed that an improvement of CTV-T_{HR} DVH parameters in advanced gynecological tumors, where the need for IC/IS BT is mandatory, could be achieved with the help of individualized 3D-printed applicators without exceeding the dose

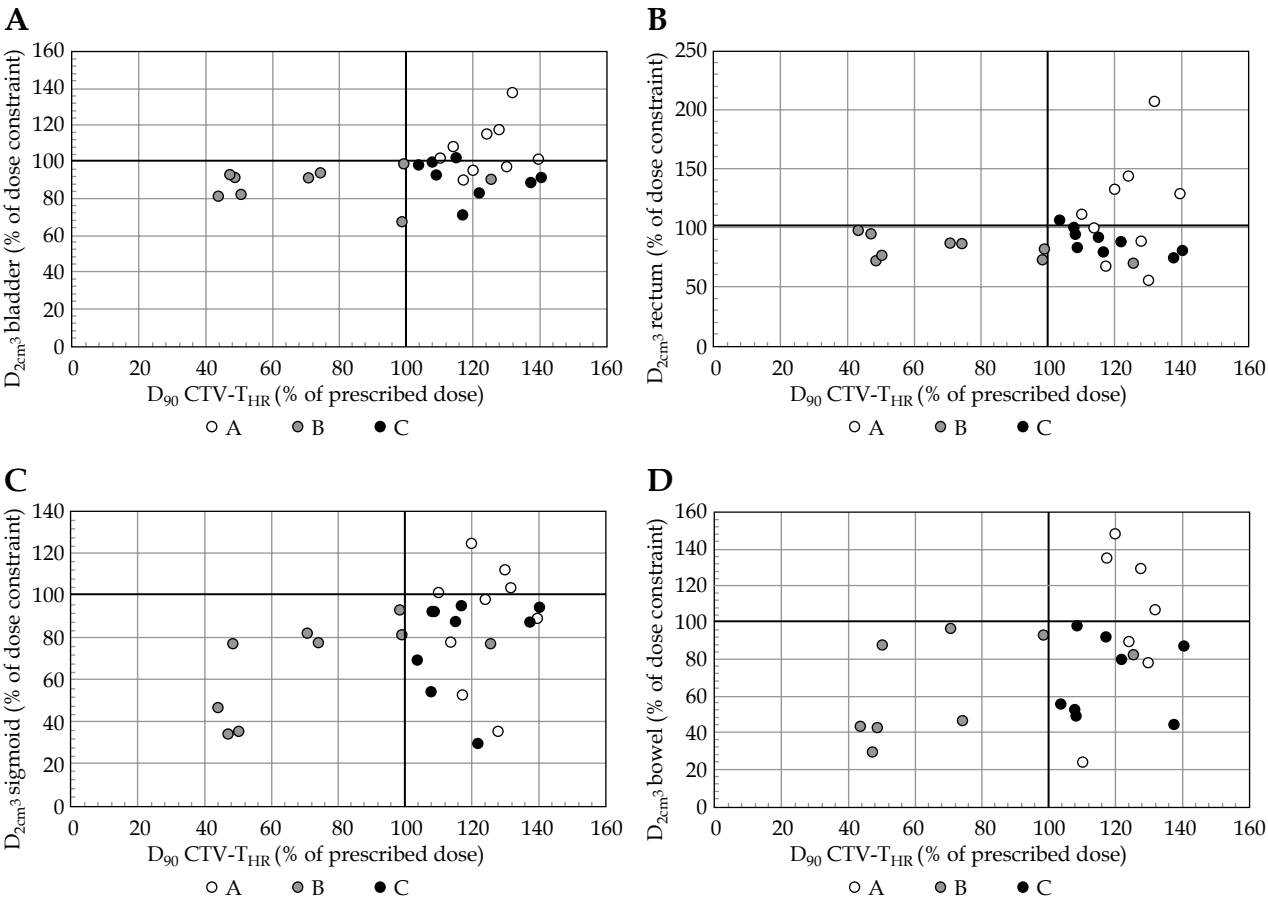

Fig. 5. A-D) Relation between percentage of the dose constraints to OARs and percentage of prescribed dose to D_{90} CTV-T_{HR} for plan A, B, and C for D_{2cm^3} **A**) bladder; **B**) rectum; **C**) sigmoid and **D**) bowel. Assuming an EBRT dose of 45 (50) Gy with 1.8 (2) Gy/fraction, the D_{2cm^3} constraints for a single BT fraction are 15.1 (12.5) Gy for bladder and 13.4 (10.6) Gy for rectum, sigmoid, and bowel. DVH constraints are indicated with horizontal and vertical black line

to OARs. A higher D_{90} can result in better tumor control probability. However, long-term results with regard to local control and survival should be evaluated in further studies, preferably with a larger number of patients.

Acknowledgements

We would like to thank Assoc. Prof. Igor Drstvenšek from the University of Maribor, Faculty of Mechanical Engineering for his contribution in designing and manufacturing individual applicators.

Disclosure

Authors report no conflict of interest.

References

1. Sturdza A, Pötter R, Ulrik Fokdal L et al. Image guided brachytherapy in locally advanced cervical cancer: Improved pelvic control and survival in RetroEMBRACE, a multicenter cohort study. *Radiother Oncol* 2016; 120: 428-433.
2. Lindegaard JC, Tanderup K, Kynde Nielsen S et al. MRI-guided 3D optimization significantly improves DVH parameters of pulsed-dose-rate brachytherapy in locally advanced cervical cancer. *Int J Radiat Oncol Biol Phys* 2008; 71: 756-764.
3. Tanderup K, Nielsen SK, Nyvang GB et al. From point A to the sculpted pear: MR image guidance significantly improves tumour dose and sparing of organs at risk in brachytherapy of cervical cancer. *Radiother Oncol* 2010; 94: 173-180.
4. Pötter R, Georg P, Dimopoulos JCA et al. Clinical outcome of protocol based image (MRI) guided adaptive brachytherapy combined with 3D conformal radiotherapy with or without chemotherapy in patients with locally advanced cervical cancer. *Radiother Oncol* 2011; 100: 116-123.
5. Charra-Brunaud C, Harter V, Delannes M et al. Impact of 3D image-based PDR brachytherapy on outcome of patients treated for cervix carcinoma in France: Results of the French STIC prospective study. *Radiother Oncol* 2012; 103: 305-313.
6. Kirisits C, Lang S, Dimopoulos J et al. The Vienna applicator for combined intracavitary and interstitial brachytherapy of cervical cancer: Design, application, treatment planning, and dosimetric results. *Int J Radiat Oncol Biol Phys* 2006; 65: 624-630.
7. Dimopoulos JCA, Kirisits C, Petric P et al. The Vienna applicator for combined intracavitary and interstitial brachytherapy of cervical cancer: clinical feasibility and preliminary results. *Int J Radiat Oncol Biol Phys* 2006; 66: 83-90.
8. Fokdal L, Tanderup K, Hokland SB et al. Clinical feasibility of combined intracavitary/interstitial brachytherapy in locally advanced cervical cancer employing MRI with a tandem/ring applicator in situ and virtual preplanning of the interstitial component. *Radiother Oncol* 2013; 107: 63-68.

9. Fokdal L, Sturdza A, Mazeron R et al. Image guided brachytherapy in cervical cancer with combined intracavitary and interstitial technique improves the therapeutic ratio in locally advanced cervical cancer: Analysis from the retro-EMBRACE study. *Radiother Oncol* 2016; 120: 434-440.
10. Nomden CNS, De Leeuw AAC, Moerland MA et al. Clinical use of the Utrecht applicator for combined intracavitary/interstitial brachytherapy treatment in locally advanced cervical cancer. *Radiat Oncol Biol* 2012; 82: 1424-1430.
11. Jürgenliemk-Schulz IM, Tersteeg RJHA, Roesink JM et al. MRI-guided treatment-planning optimisation in intracavitary or combined intracavitary/interstitial PDR brachytherapy using tandem ovoid applicators in locally advanced cervical cancer. *Radiother Oncol* 2009; 93: 322-330.
12. Mohamed S, Kallehauge J, Fokdal L et al. Parametrial boosting in locally advanced cervical cancer: Combined intracavitary/interstitial brachytherapy vs. intracavitary brachytherapy plus external beam radiotherapy. *Brachytherapy* 2015; 14: 23-28.
13. Tanderup K, Fokdal LU, Sturdza A et al. Effect of tumor dose, volume and overall treatment time on local control after radiochemotherapy including MRI guided brachytherapy of locally advanced cervical cancer. *Radiother Oncol* 2016; 120: 441-446.
14. Lindegaard JC, Madsen MLL, Traberg A et al. Individualised 3D printed vaginal template for MRI guided brachytherapy in locally advanced cervical cancer. *Radiother Oncol* 2016; 118: 173-175.
15. Sethi R, Cunha A, Mellis K et al. Clinical applications of custom-made vaginal cylinders constructed using three-dimensional printing technology. *J Contemp Brachytherapy* 2016; 8: 208-214.
16. Poulin E, Gardi L, Fenster A et al. Ultrasound in HDR brachytherapy: Towards real-time 3D ultrasound planning and personalized 3D printing for breast HDR brachytherapy treatment. *Radiother Oncol* 2015; 114: 335-338.
17. Ricotti R, Vavassori A, Bazani A et al. 3D-printed applicators for high dose rate brachytherapy: Dosimetric assessment at different infill percentage. *Phys Medica* 2016; 32: 1698-1706.
18. Jones EL, Baldion AT, Thomas C et al. Skin Introduction of novel 3D-printed superficial applicators for high-dose-rate skin brachytherapy. *Brachytherapy* 2017; 16: 409-414.
19. Canters RA, Lips IM, Wendling M et al. Clinical implementation of 3D printing in the construction of patient specific bolus for electron beam radiotherapy for non-melanoma skin cancer. *Radiother Oncol* 2016; 121: 148-153.
20. Zobec Logar BH, Hudej R. EP-1978: Individualized approach to brachytherapy in cervical cancer patient: a case report study. *Radiother Oncol* 2016; 119: S936-937.
21. Sekii S, Tsujino K, Kosaka K et al. Inversely designed, 3D-printed personalized template-guided interstitial brachytherapy for vaginal tumors. *J Contemp Brachytherapy* 2018; 10: 470-477.
22. Huang MW, Zhang JG, Zheng L et al. Accuracy evaluation of a 3D-printed individual template for needle guidance in head and neck brachytherapy. *J Radiat Res* 2016; 57: 662-667.
23. Rijkmans E, Nout R, Rutten I et al. Improved survival of patients with cervical cancer treated with image-guided brachytherapy compared with conventional brachytherapy. *Gynecol Oncol* 2014; 135: 231-238.
24. Mazeron R, Castelnau-Marchand P, Dumas I et al. Impact of treatment time and dose escalation on local control in locally advanced cervical cancer treated by chemoradiation and image-guided pulsed-dose rate adaptive brachytherapy. *Radiother Oncol* 2015; 114: 257-263.
25. Dimopoulos JCA, Pötter R, Lang S et al. Dose–effect relationship for local control of cervical cancer by magnetic resonance image-guided brachytherapy. *Radiother Oncol* 2009; 93: 311-315.
26. Ribeiro I, Janssen H, De Brabandere M et al. Long term experience with 3D image guided brachytherapy and clinical outcome in cervical cancer patients. *Radiother Oncol* 2016; 120: 447-454.
27. Tinkle CL, Weinberg V, Chen LM et al. Inverse planned high-dose-rate brachytherapy for locoregionally advanced cervical cancer: 4-year outcomes. *Int J Radiat Oncol Biol Phys* 2015; 92: 1093-1100.
28. Rogelj P, Baraković M. Cervix cancer spatial modelling for brachytherapy applicator analysis. *Informatica* 2015; 39: 261-269.
29. Hellebust TP, Kirisits C, Berger D et al. Recommendations from Gynaecological (GYN) GEC-ESTRO Working Group: considerations and pitfalls in commissioning and applicator reconstruction in 3D image-based treatment planning of cervix cancer brachytherapy. *Radiother Oncol* 2010; 96: 153-160.
30. Cunha J, Mellis K, Sethi R et al. Evaluation of PC-ISO for customized, 3D printed, gynecologic 192 Ir HDR brachytherapy applicators. *J Appl Clin Med Phys* 2015; 16: 246-253.
31. Walker JM, Elliott DA, Kubicky CD et al. Manufacture and evaluation of 3-dimensional printed sizing tools for use during intraoperative breast brachytherapy. *Adv Radiat Oncol* 2016; 1: 132-135.
32. Castelnau-Marchand P, Chargari C, Maroun P et al. Clinical outcomes of definitive chemoradiation followed by intracavitary pulsed-dose rate image-guided adaptive brachytherapy in locally advanced cervical cancer. *Gynecol Oncol* 2015; 139: 288-294.
33. Pötter R, Tanderup K, Kirisits C et al. The EMBRACE II study: The outcome and prospect of two decades of evolution within the GEC-ESTRO GYN working group and the EMBRACE studies. *Clin Transl Radiat Oncol* 2018; 9: 48-60.
34. Lindegaard JC, Fokdal LU, Nielsen SK et al. MRI-guided adaptive radiotherapy in locally advanced cervical cancer from a Nordic perspective. *Acta Oncol (Madr)* 2013; 52: 1510-1519.
35. Mazeron R, Fokdal LU, Kirchheiner K et al. Image guided brachytherapy in cervical cancer Dose–volume effect relationships for late rectal morbidity in patients treated with chemoradiation and MRI-guided adaptive brachytherapy for locally advanced cervical cancer: Results from the prospective multi. *Radiother Oncol* 2016; 120: 412-419.
36. Mazeron R, Maroun P, Castelnau-Marchand P et al. Pulsed-dose rate image-guided adaptive brachytherapy in cervical cancer: Dose–volume effect relationships for the rectum and bladder. *Radiother Oncol* 2015; 116: 226-232.
37. Fokdal L, Tanderup K, Nielsen SK et al. Image and laparoscopic guided interstitial brachytherapy for locally advanced primary or recurrent gynaecological cancer using the adaptive GEC ESTRO target concept. *Radiother Oncol* 2011; 100: 473-479.
38. Mahantshetty U, Shrivastava S, Kalyani N et al. Template-based high-dose-rate interstitial brachytherapy in gynecologic cancers: a single institutional experience. *Brachytherapy* 2014; 13: 337-342.
39. Kubicek GJ, Xue J, Xu Q et al. Stereotactic body radiotherapy as an alternative to brachytherapy in gynecologic cancer. *Biomed Res Int* 2013; 2013: 1-6.
40. Gemignani ML, Alektiar KM, Leitao M et al. Radical surgical resection and high-dose intraoperative radiation therapy (HDR-IORT) in patients with recurrent gynecologic cancers. *Int J Radiat Oncol Biol Phys* 2001; 50: 687-694.